New high temperature modification of CeTiGe: structural characterization and physical properties

2010 J. Phys.: Condens. Matter 22 146003

(http://iopscience.iop.org/0953-8984/22/14/146003)

J. Phys.: Condens. Matter **22** (2010) 146003 (6pp) doi:10.1088/0953-8984/22/14/146003

New high temperature modification of CeTiGe: structural characterization and physical properties

B Chevalier[1], W Hermes[2], E Gaudin[1,3] and R Pöttgen[2]

[1] CNRS, Université de Bordeaux, ICMCB, 87 avenue du Docteur Albert Schweitzer, 33608 Pessac Cedex, France
[2] Institut für Anorganische und Analytische Chemie, Westfälische Wilhelms-Universität Münster, Corrensstraße 30, 48149 Münster, Germany

E-mail: gaudin@icmcb-bordeaux.cnrs.fr

Received 15 November 2009, in final form 26 January 2010
Published 17 March 2010
Online at stacks.iop.org/JPhysCM/22/146003

Abstract
The new high temperature form (HT) of the ternary germanide CeTiGe was prepared by annealing at 1373 K. The investigation of HT-CeTiGe by x-ray powder diffraction shows that the compound crystallizes in the tetragonal CeScSi type structure (space group $I4/mmm$; $a = 414.95(2)$ and $c = 1590.85(10)$ pm as unit cell parameters). Electrical resistivity, thermoelectric power, magnetization and specific heat measurements performed down to 2 K on HT-CeTiGe reveal a non-magnetic strongly correlated electron system; the specific heat divided by temperature attains a value of 0.635 J mol^{-1} K^{-2} at 2 K. The comparison of the physical properties of the two crystallographic modifications of CeTiGe suggests a decrease of the hybridization J_{cf} between 4f(Ce) and conduction electrons in the sequence LT-CeTiGe (CeFeSi type) $\rightarrow$ HT-CeTiGe (CeScSi type).

1. Introduction

Intermetallic cerium compounds have attracted considerable attention among solid state chemists and physicists since they exhibit a variety of interesting physical properties (Kondo ferromagnetism, superconductivity, magnetically or non-magnetically ordered heavy-fermion system, Kondo type behaviour, etc) which are directly related to J_{cf} hybridization between the conduction and 4f(Ce) electrons. Among this large family of compounds, the equiatomic CeTX intermetallics (T = transition metal and X = element of the third, fourth, or fifth main group) have been most intensively investigated. Outstanding examples are CeNiIn, CeNiSn, CePtSn, or CeRhSb for which already more than 380 entries occur in the current SciFinder Scholar version[4].

While most of the around 100 CeTX intermetallics exhibit only one polymorphic form, a few CeTX compounds show structural phase transitions as a function of temperature or pressure. Tiny changes occur in the structures of α- and β-CeCuSn [1]. The ordered Cu_3Sn_3 hexagons reveal different degrees of puckering in the high (HT) and low (LT) temperature modifications. The structural changes are more drastic in the modifications of CeRhGe and $Ce(Rh_{0.69}Ir_{0.31})Ge$ [2–4]. The three-dimensional [Rh(Ir)Ge] polyanion shows significantly different tilting around 500–520 K and 236–258 K, respectively, and this is accompanied by a drastic jump in the magnetic susceptibility in the same temperature range [2, 3]. For instance for CeRhGe, the lattice parameters are $a = 723.0$, $b = 446.2$ and $c = 740.8$ pm at 530 K and $a = 742.9$, $b = 446.7$ and $c = 712.1$ pm at room temperature, showing a strong increase of a and consequently an important decrease of c [4]. The phase transitions occurring in CeCuSn and CeRhGe are of a displacive type.

Temperature driven reconstructive phase transitions occur for CePdZn [5], CeNiGa [6] and CePdAl [7], but with a different sequence of the structure types, i.e. α-CePdZn or α-CeNiGa with hexagonal ZrNiAl type and β-CePdZn or β-CeNiGa with the orthorhombic TiNiSi type, while α-CePdAl adopts a new orthorhombic structure type and β-CePdAl crystallizes with the hexagonal ZrNiAl type. Thus, tiny

[3] Author to whom any correspondence should be addressed.
[4] 23 entries occur for the formula CeNiIn, 224 for CeNiSn, 52 for CePtSn, and 88 for CeRhSb in the SciFinder Scholar version 2009: http://www.cas.org/SCIFINDER/SCHOLAR/.

differences in the atom sizes and the electronic structure force different crystal structures. This has large influence on the physical properties, e.g. one observes stronger 4f(Ce)–4d(Pd) hybridization in α-CePdZn [5]. One of the most peculiar examples is the static mixed-valent stannide CeRuSn [8, 9] which exhibits an ordering of trivalent and intermediate-valent cerium and undergoes a phase transition to a modulated structure at low temperatures.

The structural phase transitions reported for CeRhAs [10], CePdSn [11], CePtSn [12], and CeAuGe [13] are pressure induced. The most interesting example is certainly observed for CeRhAs, which shows successive structural phase transitions at 360, 235, and 165 K with drastic drops in the lattice parameters [10]. CePdSn and CePtSn show reconstructive phase transitions with orthorhombic TiNiSi type low- and hexagonal ZrNiAl type high-pressure modifications [11, 12]. CeAuGe was studied under *in situ* conditions in a diamond anvil cell. At 8.7(7) GPa a first order phase transition from a hexagonal NdPtSb type to an orthorhombic TiNiSi type occurs [13].

During our systematic studies on structure–property relationships of CeTX intermetallics, we study such compounds under different temperature and pressure conditions in order to elucidate possible phase transitions which might results in interesting physical properties changes. In this context we were interested in the ternary germanide CeTiGe, which was first reported by Welter *et al* [14] and Morozkin *et al* [15, 16]. The samples obtained by arc melting followed by an annealing at 1180–1273 K crystallize with the tetragonal CeFeSi type, space group $P4/nmm$. CeTiGe with this low temperature form (LT) is a non-magnetically ordered heavy-fermion system showing an enhanced Sommerfeld coefficient $\gamma \approx 0.3$ J K^{-2} mol^{-1} [17]. Isotypic GdTiGe [18] shows temperature driven dimorphism with drastic changes in the magnetic properties; the two modifications are respectively ferromagnetically ($T_C = 376$ K) and antiferromagnetically ($T_N = 412$ K) ordered. Keeping these results in mind, we reinvestigated CeTiGe and observed a new high temperature form (HT) with tetragonal CeScSi type structure, space group $I4/mmm$. Herein we report on our crystal chemical results and discuss the physical properties changes between the two forms (LT and HT).

2. Experimental details

Starting materials for the synthesis of HT-CeTiGe were a cerium ingot (Johnson Matthey), titanium sponge (Degussa-Hüls, about 200 mesh), and germanium granules (Merck), all with a stated purity better than 99.9%. Pieces of the cerium ingot were first arc melted into small buttons under purified argon using molecular sieves, silica gel and titanium sponge heated at 900 K. The Ce, Ti and Ge elements were then weighed in the 32.5:34.5:33.0 atomic ratio. The elements were arc melted under a purified argon pressure of about 700 mbar. The resulting button was turned over and remelted three times in order to ensure homogeneity. The regulus was then crushed under n-hexane and ground. The resulting powder was cold-pressed to a small pellet ($\varnothing = 6$ mm) and sealed in a small tantalum crucible under an argon pressure of about 600 mbar. The arc welded closed tantalum ampoule was placed in the water-cooled sample chamber of an induction furnace (Hüttinger Elektronik, Freiburg, Typ TIG 1.5/300) rapidly heated to 1373 K and kept at that temperature for approximately 1 h; the temperature was controlled by a Sensor Therm Metis MS09 pyrometer with an accuracy of $\pm$30 K. Then the temperature was lowered by 10 K h^{-1} to 1273 K and finally the sample was quenched by switching off the power supply.

The same synthesis procedure applied to the starting composition 33.3:33.3:33.3 as atomic ratio leads to a product containing a small amount of the ferromagnetic binary germanide Ce_5Ge_3 ($T_C = 6.4$ K) [19]. In order to inhibit the presence of Ce_5Ge_3 in the final sample, the starting composition was slightly modified as indicated above. These considerations were made using the phase equilibria in the Ce–Ti–Ge system [20]. Finally, we should note that simply arc-melted samples result in the formation of mainly Ti_5Ge_3, Ce_5Ge_3, Ti and LT-CeTiGe, indicating peritectic formation of the HT-CeTiGe phase.

The crystal structure of the ternary germanide HT-CeTiGe was determined using x-ray powder diffraction. In order to minimize problems of preferred orientation of the crystallites, a finely ground (<40 μm) powder of the sample was randomly scattered over a substrate made of the same sample. The data were collected with a Philips X-Pert diffractometer operating at room temperature and using Cu Kα radiation. The powder diffraction pattern was scanned over the angular range 15.011°–119.986° with a step size of $\Delta(2\theta) = 0.017°$. Rietveld refinement (figure 1) was performed using the Jana2006 program package [21]. The background was estimated by a Legendre function, and the peak shapes were described by a pseudo-Voigt function. The cell parameters of the tetragonal cell were refined to the values $a = 414.95(2)$ and $c = 1590.85(10)$ pm. Three impurity phases were taken into account for the refinement e.g. LT-CeTiGe [16], Ti_5Ge_3 [22] and Ce_5Ge_3 [23]. The atomic parameters for these three phases were fixed to the values reported in the literature; only the cell parameters were refined. For HT-CeTiGe, the initial atomic coordinates were taken from the previous study of the isotypic ternary germanide GdTiGe adopting the tetragonal CeScSi type [18]. An absorption correction and a preferential orientation along the [110] direction were introduced. The final refinement of the atomic positions with isotropic atomic displacement parameters (ADPs) led to the profile factors $R_p/R_{wp} = 4.95/6.68\%$ and the Bragg factor $R_B(\text{obs}) = 5.81\%$. The final atomic positions and isotropic ADPs are gathered in table 1. The refined amounts of impurities were equal to 19.2(8), 2.5(4) and 1.1(9) wt% for LT-CeTiGe, Ti_5Ge_3 and Ce_5Ge_3, respectively. The two last compounds Ti_5Ge_3 and Ce_5Ge_3 are respectively non-magnetic [22] and ferromagnetic [19]. Also, these impurities were localized using scanning electron microscopy in the grain boundaries.

Magnetization measurements were performed using a superconducting quantum interference device (SQUID) magnetometer in the temperature range 2–300 K and applied

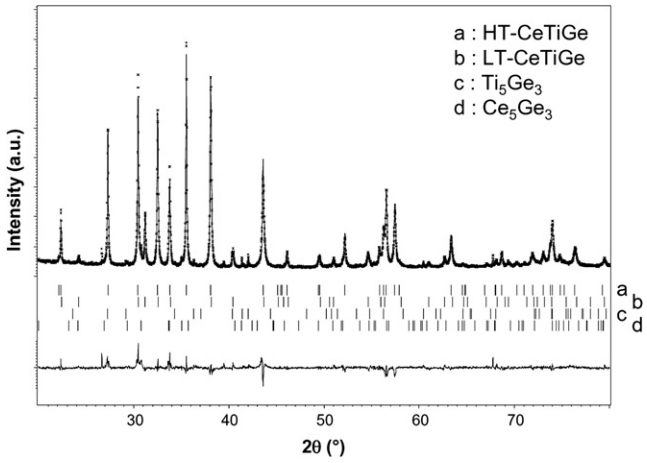

Figure 1. Rietveld profile refinement of the x-ray diffraction pattern of the HT-CeTiGe sample at $T = 293$ K ($\lambda = 1.54051$ Å). The bottom vertical bars correspond to the Bragg peak positions for the main phase and the three impurities.

Table 1. Atomic coordinates and isotropic displacement parameters (Å^2) for LT-CeTiGe [16] ($a = 412.8(1)$ and $c = 790.8(1)$ pm) and HT-CeTiGe ($a = 414.95(2)$ and $c = 1590.85(10)$ pm).

Atom	Wyckoff site	x	y	z	U_{eq}
LT-CeTiGe, $P4/nmm$					
Ce	2*c*	1/4	1/4	0.649(3)	—
Ti	2*a*	3/4	1/4	0	—
Ge	2*c*	1/4	1/4	0.227(6)	—
HT-CeTiGe, $I4/mmm$					
Ce	4*e*	0	0	0.3262(2)	0.0159(14)
Ti	4*c*	0	1/2	0	0.026(4)
Ge	4*e*	0	0	0.1151(5)	0.019(2)

fields up to 3 T and a PPMS (Quantum Design). The measurement of the electrical resistivity was carried out above 4.2 K on a bar of 1.5 × 1.5 × 5 mm^3, using a standard dc four probe method, with silver paint contacts and an intensity current of 10 mA. Due to the presence of microcracks in the sample, the absolute value of ρ could not be determined accurately; for this reason, a reduced representation $\rho(T)/\rho(270\ \text{K})$ is chosen. Thermoelectric power measurements were performed on the bar previously described using a dynamic method. Details of the cell used and of the measurement methods have been described previously [24]. Heat capacity measurements were realized by a relaxation method with a Quantum Design PPMS system and using a two tau model analysis.

3. Results and discussion

Using the unit cell parameters reported in table 1, it is observed that the molar volume of HT-CeTiGe (0.0685 nm^3) is weakly higher than that existing for LT-CeTiGe (0.0674 nm^3). This observation suggests that the chemical bonding between 4f(Ce) states and its ligands is smaller in the HT-CeTiGe phase. Also, this last phase adopts the same structure as CeScGe [25]

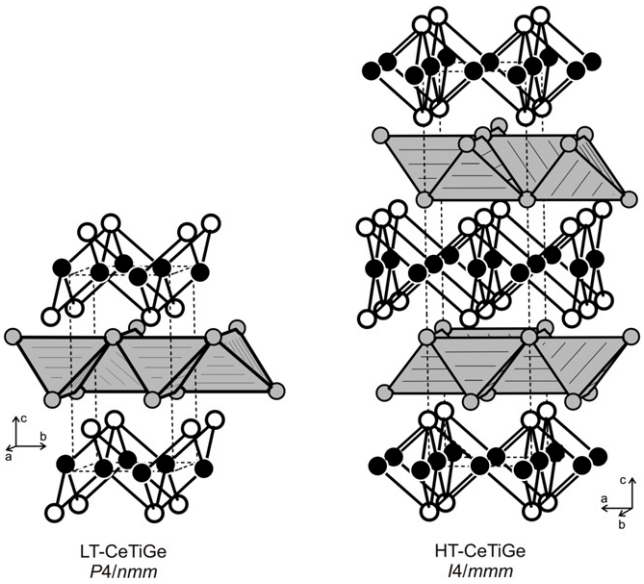

Figure 2. The crystal structures of LT-CeTiGe and HT-CeTiGe. Cerium, titanium, and germanium atoms are drawn as medium grey, black filled, and open circles, respectively. The empty condensed Ce_4 tetrahedra and the Ti–Ge coordination are emphasized. For details see the text.

Table 2. Number of neighbours and interatomic distances (pm) in the structures of LT-CeTiGe [16] and HT-CeTiGe. Standard deviations are all equal or less than 0.3 pm.

LT-CeTiGe				HT-CeTiGe			
Ce:	4	Ge	307.2	Ce:	4	Ge	307.9
	1	Ge	336.1		1	Ge	335.8
	4	Ti	344.0		4	Ti	345.7
	4	Ce	378.1		4	Ce	380.6
	4	Ce	412.8		4	Ce	414.9
Ti:	4	Ge	273.5	Ti:	4	Ge	276.7
	4	Ti	291.9		4	Ti	293.4
	4	Ce	344.0		4	Ce	345.7
Ge:	4	Ti	273.5	Ge:	4	Ti	276.7
	4	Ce	307.2		4	Ce	307.9
	1	Ce	336.1		1	Ce	335.8

but its molar volume is smaller (0.0740 nm^3 for CeScGe) in agreement with the evolution of the metallic radius from Ti (146.2 pm) to Sc (164.1 pm).

CeTiGe is a further example for temperature driven polymorphism. The CeFeSi type low temperature modification has already been described in [14, 16]. Herein we focus on a crystal chemical comparison with the high temperature form (CeScSi type) which forms upon a reconstructive phase transition. Views on both modifications are presented in figure 2. The cerium atoms in LT- and HT-CeTiGe built up layers of empty edge-sharing Ce_4 tetrahedra which are separated by the titanium–germanium networks. The cerium atoms in both modifications have eight cerium neighbours (table 2). As expected, the Ce–Ce distances are slightly longer in the HT-modification. The Ce–Ce distances are all well above the Hill limit [26] of about 340 pm for 4f(Ce) electron localization, so that sufficient localization for the onset of ordered magnetic moments can be expected.

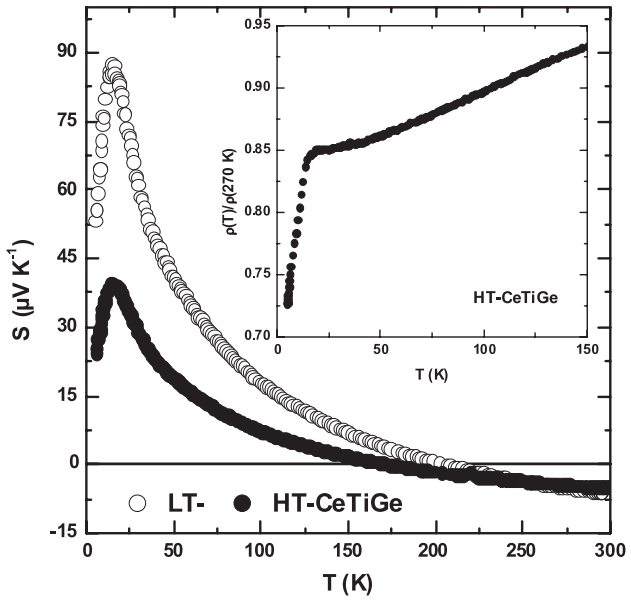

Figure 3. Temperature dependence of the thermoelectric power S for LT- and HT-CeTiGe. The inset presents the dependence of the reduced electrical resistivity versus T for HT-CeTiGe.

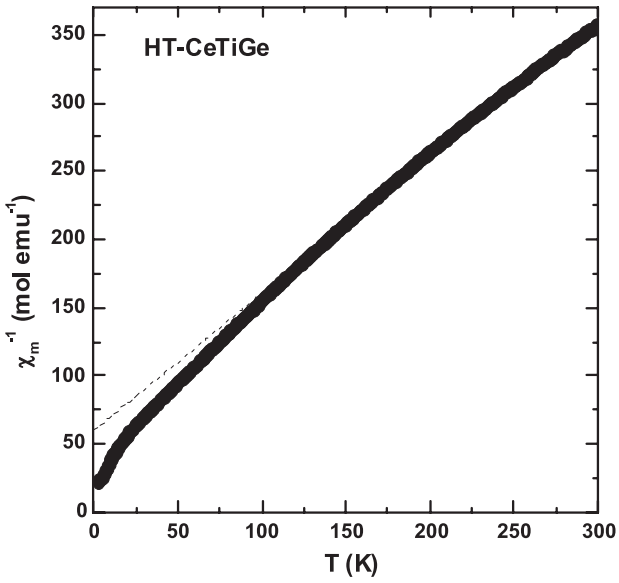

Figure 4. Temperature dependence of the reciprocal magnetic susceptibility χ_m^{-1} measured for an applied field $H = 3$ T for HT-CeTiGe.

The striking structural difference between both modifications concerns the [TiGe] networks. The titanium atoms in both modifications have four germanium neighbours, in tetrahedral coordination in LT-CeTiGe but in a planar coordination in HT-CeTiGe. The Ti–Ge distances in both modifications of 274 pm (LT) and 277 pm (HT) are both longer than the sum of the covalent radii [27] of 254 pm, indicating only weak Ti–Ge bonding. In contrast, both modifications show short Ti–Ti distances of 292 (LT) and 293 pm (HT), which compare well with the Ti–Ti distances (6 × 290 and 6 × 295 pm) in hcp titanium [28]. Similar to the many ZrCuSiAs type materials [29], also in the two modifications of CeTiGe we observe substantial Ti–Ti bonding.

The centres of the Ce_4 tetrahedra in both modifications are special positions, i.e. Wyckoff site 2*d* (1/4 3/4 1/2) in LT-CeTiGe and 4*d* (0 1/2 1/4) in HT-CeTiGe. These empty tetrahedra are favourable for hydrogenation, as recently demonstrated for the isotypic compound CeRuSi and its hydride CeRuSiH [30]. Filling of Ce_4 tetrahedral sites with hydrogen without cell expansion for both forms of CeTiGe would lead to Ce–H distances of 238 (LT) and 240 pm (HT), which are comparable to the ones in the structurally related hydrides CeRuSiH (244.7 pm) [30] and CeCoSiH (239.1 pm) [31]. Our recent hydrogenation experiments on LT-CeTiGe and HT-CeTiGe resulted in the hydride CeTiGeH adopting a structure derivative from the CeScSi type; these results will be reported in a forthcoming paper.

The temperature dependence of the reduced electrical resistivity $\rho(T)/\rho(270\ \mathrm{K})$ of HT-CeTiGe, is shown in the inset of the figure 3. In the temperature range 270–38 K, the resistivity decreases almost linearly with the lowering of temperature, then decreases weakly between 38 and 15 K, and finally a sudden change of slope is detected at 15(1) K on the curve $\rho(T)/\rho(270\ \mathrm{K})$ versus T. This behaviour is comparable to that reported for LT-CeTiGe [17]. The decrease of the reduced resistivity occurring below 15(1) K can be attributed to the formation of the coherent Kondo lattice.

Figure 3 compares the temperature dependence between 4.2 and 300 K of the thermoelectric power S of the two modifications of CeTiGe. The curve S versus T for LT-CeTiGe exhibits the same characteristics as that determined recently, but the measured maximum value of $S = 88\ \mu\mathrm{V\ K^{-1}}$ is higher than the one reported in the literature [17]. This curve, which shows many similarities to that measured for the isotypic ternary silicide CeRuSi [30], can be explained with a model describing the influence of the crystalline field effect on the Kondo effect at temperatures larger than the Kondo temperature within the Coqblin–Schrieffer Hamiltonian for the $4f^1$ configuration of cerium [32]. The comparison between the curves S versus T concerning HT- and LT-CeTiGe indicates that for the former modification: (i) a smaller value of $S = 40\ \mu\mathrm{V\ K^{-1}}$ for the maximum and also (ii) a smaller temperature ($\cong$170 K) where S changes its sign from negative to positive with decreasing temperature. The comparison suggests that the influence of the Kondo effect on the physical properties of CeTiGe decreases in the sequence LT-CeTiGe → HT-CeTiGe. A similar decrease of the S value for the maximum of the curve S versus T is evidenced in the system $Ce(Ni_xPd_{1-x})_2Si_2$ [33] and in $CePd_2Si_2$ when external pressure is applied [34]. In other words, the temperature dependence of S in the sequence LT-CeTiGe → HT-CeTiGe reveals a decrease of the hybridization between the 4f(Ce) and the conduction electrons.

Above 100 K, the temperature dependence of the reciprocal magnetic susceptibility χ_m^{-1} of HT-CeTiGe (figure 4) can be fitted with a Curie–Weiss law $\chi_m^{-1} = (T - \theta_p)/C_m$ giving $\theta_p = -59(2)$ K as the paramagnetic Curie temperature and $\mu_{eff} = (8C_m)^{1/2} = 2.60(5)\ \mu_B\ \mathrm{mol^{-1}}$ as the effective paramagnetic moment, a value close to that calculated for

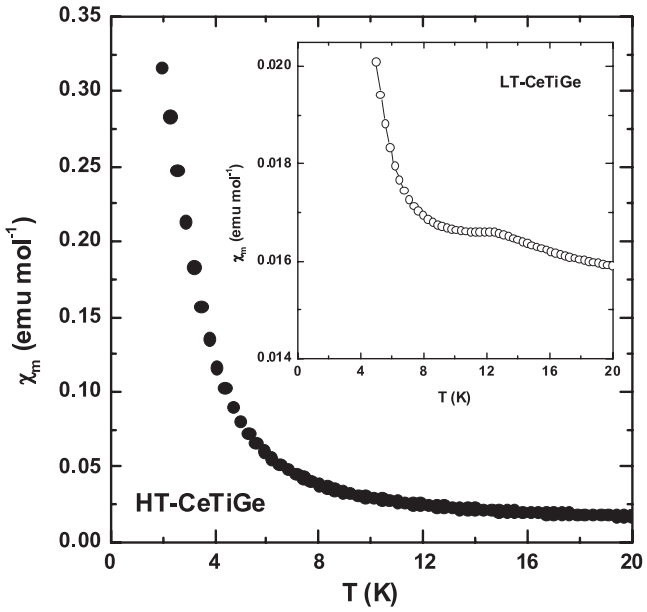

Figure 5. Temperature dependence of the magnetic susceptibility χ_m measured for an applied field $H = 0.1$ T for HT-CeTiGe. The inset presents the curve χ_m versus T for LT-CeTiGe.

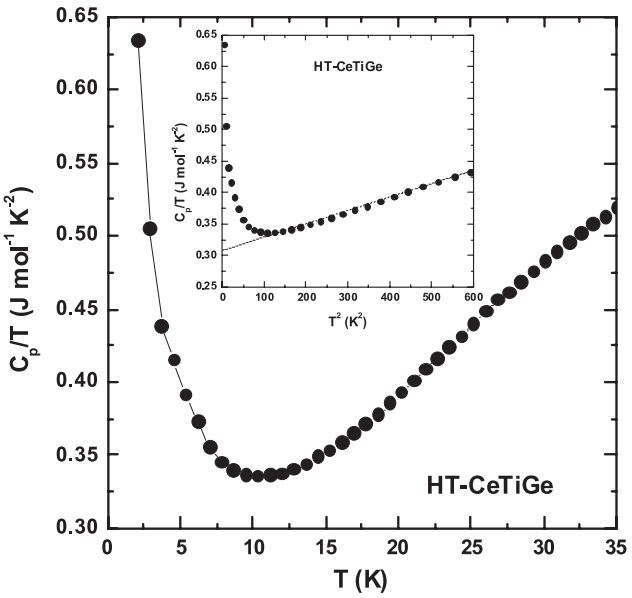

Figure 6. Temperature dependence of the specific heat C_p divided by temperature for HT-CeTiGe (the line is a guide for eye). The inset presents the curve C_p/T versus T^2.

the free Ce^{3+} ion ($\mu_{eff} = 2.54\ \mu_B\ mol^{-1}$). The negative curvature observed at low temperatures in the χ_m^{-1} versus T curve indicates the presence of a crystal field effect.

Before the presentation of the magnetization and specific heat measurements performed down to 2 K (figures 5 and 6), we must mention: (i) that these data reveal no anomaly around 6.4 K attributed to the ferromagnetic transition of Ce_5Ge_3 [19], and (ii) that the impact on these data of the LT-CeTiGe phase was subtracted.

No anomaly can be detected down to 2 K from the curve χ_m versus T giving the temperature dependence of the magnetic susceptibility measured at low field $H = 0.1$ T for HT-CeTiGe (figure 5). At 2 K, χ_m takes a value of 0.316 emu mol^{-1}. This evolution of χ_m is different to that existing for LT-CeTiGe (inset of figure 5), where a shoulder appears around 10–12 K. This last anomaly detected also by Deppe *et al* [17] but at higher temperature (24 K) characterizes the spin fluctuation temperature resulting from the hybridization between the 4f(Ce) and the conduction electrons. As a similar anomaly is not observed for HT-CeTiGe, the magnetization measurement confirms the decrease of the hybridization in the sequence LT-CeTiGe → HT-CeTiGe.

Finally, the ternary germanide HT-CeTiGe was investigated by specific heat measurements (figure 6). No peak can be observed from the curve C_p/T versus T, in agreement with the absence of magnetic ordering down to 2 K as reported from the magnetization measurements. However, around 10 K, this curve exhibits a strong increase, attaining a value of 0.635 J mol^{-1} K^{-2} at 2 K, suggesting that this form is a strongly correlated electron system at low temperature. At higher temperature, between 12 and 25 K, an enhanced Sommerfeld coefficient $\gamma = 0.308$ J mol^{-1} K^{-2} can be obtained by fitting the data C_p/T versus T^2 (inset of figure 6). This γ value is comparable to that reported for LT-CeTiGe [17] but the specific heat of this last form does not show an increase at low temperature.

4. Conclusion

The magnetization, electrical resistivity, thermoelectric power, and specific heat measurements presented here for HT-CeTiGe indicate that this compound does not show magnetic ordering down to 2 K. However, this study reveals at low temperatures some characteristic features of a non-magnetic strongly correlated electron system: an important increase of its magnetic susceptibility and specific heat. Also, these results suggest that the physical properties of CeTiGe are strongly dependent on its structural properties; the 4f(Ce)–conduction electrons interaction decreases from the low temperature form (CeFeSi type) to the high temperature form (CeScSi type). A detailed investigation of the Ce–Ti–Ge system near the CeTiGe composition is now in progress in order to explain these different behaviours.

Acknowledgments

This work was financially supported by the Deutsche Forschungsgemeinschaft. BC, EG and RP are indebted to EGIDE and DAAD for research grants within the PROCOPE programs (11457RD and D/0502176). WH is indebted to the Fonds der Chemischen Industrie and the NRW Graduate School of Chemistry for a PhD stipend. Finally, BC thanks the European Science Foundation (ECOM-COST action P16) for financial support.

References

[1] Sebastian C P, Rayaprol S, Hoffmann R-D, Rodewald U Ch, Pape T and Pöttgen R 2007 *Z. Naturforsch.* b **62** 647

[2] Ueda T, Honda D, Shiromoto T, Metoki N, Honda F, Kaneko K, Haga Y, Matsuda T D, Takeuchi T, Thamizhavel A, Sugiyama K, Kindo K, Settai R and Ōnuki Y 2005 *J. Phys. Soc. Japan* **74** 2836

[3] Gaudin E, Chevalier B, Heying B, Rodewald U Ch and Pöttgen R 2005 *Chem. Mater.* **17** 2693

[4] Hermes W, Hoffmann R-D, Chevalier B, Gaudin E and Pöttgen R, unpublished results

[5] Hermes W, Mishra R, Müller H, Johrendt D and Pöttgen R 2009 *Z. Anorg. Allg. Chem.* **635** 660

[6] Chevalier B, Bobet J-L, Gaudin E, Pasturel M and Etourneau J 2002 *J. Solid State Chem.* **168** 28

[7] Gribanov A, Tursina A, Murashova E, Seropegin Y, Bauer E, Kaldarar H, Lackner R, Michor H, Royanian E, Reissner M and Rogl P 2006 *J. Phys.: Condens. Matter* **18** 9593

[8] Riecken J F, Hermes W, Chevalier B, Hoffmann R-D, Schappacher F M and Pöttgen R 2007 *Z. Anorg. Allg. Chem.* **633** 1094

[9] Matar S F, Riecken J F, Chevalier B, Pöttgen R and Eyert V 2007 *Phys. Rev.* B **76** 174434

[10] Umeo K, Masumori K, Sasakawa T, Iga T, Takabatake T, Ohishi Y and Adachi T 2005 *Phys. Rev.* B **71** 064110

[11] Heymann G, Riecken J F, Rayaprol S, Christian S, Pöttgen R and Huppertz H 2007 *Z. Anorg. Allg. Chem.* **633** 77

[12] Riecken J F, Heymann G, Soltner T, Hoffmann R-D, Huppertz H, Johrendt D and Pöttgen R 2005 *Z. Naturforsch.* b **60** 821

[13] Brouskov V, Hanfland M, Pöttgen R and Schwarz U 2005 *Z. Kristallogr.* **220** 122

[14] Welter R, Vernière A, Venturini G and Malaman B 1999 *J. Alloys Compounds* **283** 54

[15] Morozkin A V, Seropegin Yu D, Leonov A V, Sviridov I A, Tskhadadze I A and Nikitin S A 1998 *J. Alloys Compounds* **267** L14

[16] Morozkin A V, Seropegin Yu D and Sviridov I A 1999 *J. Alloys Compounds* **285** L5

[17] Deppe M, Caroca-Canales N, Hartmann S, Oeschler N and Geibel C 2009 *J. Phys.: Condens. Matter* **21** 206001

[18] Tskhadadze I A, Chernyshev V V, Streletskii A N, Portnoy V K, Leonov A V, Sviridov I A, Telegina I V, Verbetskii V N, Seropegin Yu D and Morozkin A V 1999 *Mater. Res. Bull.* **34** 1773

[19] Kurisu M, Mitsumata T and Oguro I 1999 *Physica* B **259–261** 96

[20] Morozkin A V 2004 *J. Alloys Compounds* **370** L1

[21] Petricek V, Dusek M and Palatinus L 2006 *Jana2006, The Crystallographic Computing System* (Praha: Institute of Physics)

[22] Pietrokowsky P and Duwez P 1951 *J. Met.* **3** 772
Hardy G F and Hulm J K 1954 *Phys. Rev.* **93** 1004

[23] Arbuckle J and Parthe E 1962 *Acta Crystallogr.* **15** 1205

[24] Dordor P, Marquestaut E and Villeneuve G 1980 *Rev. Phys. Appl.* **15** 1607

[25] Bodak O I and Kokhan Z M 1983 *Inorg. Mater.* **19** 987

[26] Hill H H 1970 *Plutonium and Other Actinides* (*Nuclear Materials Series* vol 17) ed W N Mines (New York: AIME) p 2

[27] Emsley J 1999 *The Elements* (Oxford: Oxford University Press)

[28] Donohue J 1974 *The Structures of the Elements* (New York: Wiley)

[29] Pöttgen R and Johrendt D 2008 *Z. Naturforsch.* b **63** 1135

[30] Chevalier B, Gaudin E, Tencé S, Malaman B, Rodriguez Fernandez J, André G and Coqblin B 2008 *Phys. Rev.* B **77** 014414

[31] Chevalier B and Matar S F 2004 *Phys. Rev.* B **70** 174408

[32] Bhattacharjee A K and Coqblin B 1976 *Phys. Rev.* B **13** 3441

[33] Huo D, Sakurai J, Maruyama O, Kuwai T and Isikawa Y 2001 *J. Magn. Magn. Mater.* **226–230** 202

[34] Link P, Jaccard D and Lejay P 1996 *Physica* B **225** 207